





In Silico and *in Vivo* Analysis of HIV-1 Rev Regulatory Protein for Evaluation of a Multiepitope-based Vaccine Candidate

Samaneh H. Shabani, Kimia Kardani, Alireza Milani & Azam Bolhassani


To cite this article: Samaneh H. Shabani, Kimia Kardani, Alireza Milani & Azam Bolhassani (2021): *In Silico* and *in Vivo* Analysis of HIV-1 Rev Regulatory Protein for Evaluation of a Multiepitope-based Vaccine Candidate, *Immunological Investigations*, DOI: [10.1080/08820139.2020.1867163](https://doi.org/10.1080/08820139.2020.1867163)


To link to this article: <https://doi.org/10.1080/08820139.2020.1867163>

 View supplementary material [↗](#)

 Published online: 08 Jan 2021.

 Submit your article to this journal [↗](#)

 Article views: 48

 View related articles [↗](#)

 View Crossmark data [↗](#)



In Silico and *in Vivo* Analysis of HIV-1 Rev Regulatory Protein for Evaluation of a Multiepitope-based Vaccine Candidate

Samaneh H. Shabani, Kimia Kardani, Alireza Milani, and Azam Bolhassani

Department of Hepatitis and AIDS, Pasteur Institute of Iran, Tehran, Iran

ABSTRACT

In silico-designed multiepitope conserved regions of human immunodeficiency virus 1 (HIV-1) proteins would be a beneficial strategy for antigen design which induces effective anti-HIV-1 T-cell responses. The conserved multiple HLA-DR-binding epitopes of Rev protein were identified using IEDB MHC-I prediction tools and SYFPEITHI webserver to screen potential T-cell epitopes. We analyzed toxicity, allergenicity, immunogenicity, hemolytic activity, cross-reactivity, cell-penetrating peptide (CPP) potency, and molecular docking of the candidate epitopes using several immune-informatics tools. Afterward, we designed a novel multiepitope construct based on non-toxic and non-allergenic Rev, Nef, Gp160 and P24-derived cytotoxic T cell (CTL) and T-helper cell (HTL) epitopes. Next, the designed construct (Nef-Rev-Gp160-P24) was subjected to three B-cell epitope prediction webserver, ProtParam and Protein-Sol to obtain the physicochemical features. Then, the recombinant multiepitope DNA and polypeptide constructs were complexed with different CPPs for nanoparticle formation and pass them via the cell membranes. Finally, the immunogenicity of multiepitope constructs in a variety of modalities was evaluated in mice. The results demonstrated that groups immunized with heterologous DNA+ MPG or HR9 CPP prime/rNef-Rev-Gp160-P24 polypeptide + LDP-NLS CPP boost regimens could significantly produce higher levels of IFN- γ and Granzyme B, and lower amounts of IL-10 than other groups. Moreover, higher levels of IgG2a and IgG2b were observed in all heterologous prime-boost regimens than homologous DNA or polypeptide regimens. Altogether, the present findings indicated that the Nef-Rev-Gp160-P24 polypeptide meets the criteria to be potentially useful as a multiepitope-based vaccine candidate against HIV-1 infection.


KEYWORDS

HIV-1; regulatory protein; multiepitope vaccine; cell-penetrating peptide; therapeutic vaccine

Introduction

Nearly 37.9 million people live with human immunodeficiency virus (HIV) in the world (HIV/AIDS Fact sheet. Available at: who.int. 2020). Development of HIV therapeutic vaccines with high potency are critical. A therapeutic vaccine needs HIV-1 antigens in a strong immunogenic context to induce potent immunity. The promising data suggest that strong T cell-mediated immunity can suppress the replication of virus and control disease progression in HIV-1 patients (Leal et al. 2017). So, the stimulation of both CD4⁺ T-cells (helper T lymphocytes; HTLs) and CD8⁺ T-cells (cytotoxic T lymphocytes; CTLs) play a main role in reduction of

CONTACT Azam Bolhassani  azam.bolhassani@yahoo.com  Department of Hepatitis and AIDS, Pasteur Institute of Iran, Tehran, Iran.

 Supplemental data for this article can be accessed on the [publisher's website](#).

© 2021 Taylor & Francis Group, LLC

HIV-1 infection (DeVico and Gallo 2004; Ranasinghe et al. 2016; Rosa et al. 2011). Due to high mutation rate of HIV-1 and multiple strains belonging to many different clades, thus it is likely that a multiepitope subunit vaccine will be necessary to stimulate broad and potent immunity (Pandey et al. 2018; Spira et al. 2003). Epitope-based vaccines target-specific epitopes within conserved regions of the pathogen (Gonzalez-Rabade et al. 2011). Therefore, these vaccines can be designed based on linear or conformational structures such as multiple-antigenic peptides containing longer peptides or minimal-length epitopes (Black et al. 2010).

Since the first determination of binding motifs for T-cell antigens by Rammensee *et al.*, epitope selection has been extensively developed by algorithms of epitope prediction (Falk et al. 1991). Some studies evaluated the development of *in silico* prediction of potential MHC class I and class II-restricted epitopes against various pathogens such as HIV-1 (Kardani et al. 2020). The fact that there is no FDA approved vaccine against HIV-1 infection make scientists to rethink about developing a potent and effective vaccine. Nowadays, new approaches such as the use of immune-informatics have been utilized in the field of vaccine design to save time and cost (Chiarella et al. 2009; Slingluff 2011). Multiepitope subunit vaccines can enhance the specificity of the target, ease in production, safety, and rate of accuracy (Sahni and Nagendra 2004; Slingluff 2011). For example, one study identified 27 conserved, multiple HLA-DR-binding peptides in HIV-1 Gag, Pol, Nef, Vif, Vpr, Rev and Vpu proteins. Mice immunization showed T-cell proliferation and subsequently IFN- γ and TNF- α secretion (Almeida et al. 2012). In another study, mice immunization with multiepitope construct harboring the 18 HIV-1 CD4⁺ epitopes induced the proliferation of T cells and the secretion of effective cytokines (Rosa et al. 2011). Fusion of the 8 HIV-1 CD4⁺ epitopes derived from P6, P17, Pol, Gp160, Rev, Vpr, Vif and Nef proteins to the heavy chain of α DEC205 efficiently enhanced immunity versus HIV-1 infection, as well (Apostólico et al. 2017). In a clinical report, the CD8⁺ T cell responses were found up to 19 and 37% of HIV-1 patients against overlapping peptides derived from Tat and Rev proteins, respectively (Addo et al. 2001). Moreover, the cellular and humoral responses were elicited in 45% of tested subjects by a peptide-based vaccine comprising a cocktail of T-cell epitopes of the conserved Rev, Vif, Vpr, and Nef sequences in a phase II clinical trial (Boffito et al. 2013).

On the other hand, the low immunogenicity of subunit antigens led to the use of improved vaccine delivery systems. Vaccine delivery systems (*e.g.*, emulsions, micro-/nanoparticles, liposomes, polymers, cell-penetrating peptides, *etc.*) mainly act to target associated antigens into antigen-presenting cells (APC) including macrophages and dendritic cells. Cell-penetrating peptides (CPPs) are imperative for antigen delivery into cellular compartments. In this line, four different types of CPPs including MPG, HR9, and CyLoP-1, LDP-NLS were used to transport different DNA and protein/peptide cargos, respectively, into eukaryotic cells (Deshayes et al. 2004; Liu et al. 2011; Ponnappan et al. 2017; Ponnappan and Chugh 2017). MPG as a short-synthesized peptide with hydrophobic and hydrophilic domains and HR9 as an arginine-rich CPP could bind non-covalently to DNA plasmids for their delivery into cells (Gros et al. 2006; Liu et al. 2011). On the other hand, CyLoP-1 as a cysteine-rich CPP and LDP-NLS as a conjugated CPP are proficient to transport protein or peptide cargos into the cells (Ponnappan et al. 2017; Ponnappan and Chugh 2017). Herein, a new multiepitope-based therapeutic vaccine candidate containing several immunodominant CTL and HTL epitopes of Nef, Rev, Gp160 and P24 proteins was developed to induce potent and effective immunity in mice. This construct was designed based on MHC I- and II-presented peptide epitopes to stimulate both CD8⁺ and CD4⁺ T-cell responses.

Our data showed that groups immunized with heterologous *nef-rev-gp160-p24* DNA+ MPG or HR9 CPP prime/rNef-Rev-Gp160-P24 polypeptide + LDP-NLS CPP boost regimens could significantly produce higher levels of IFN- γ and Granzyme B, and lower amounts of IL-10 than other groups. These designed constructs could likely induce the potent T-cell responses (Th1 response and CTL activity) as a multiepitope-based therapeutic vaccine candidate against HIV-1 infection.

Materials and methods

In silico analysis

Immunoinformatics acts as a connection between experimental immunology and computational approaches. Prediction of B- and T-cell epitopes has been the focus of immunoinformatics for a long time, given the potential translational implications, and many tools have been developed up to now. Moreover, the safety of the predicted epitopes could be determined by several servers such as allergenicity, toxicity and hemolytic prediction. Based on prediction of highly conserved epitopes such as Nef₆₀₋₇₁, Nef₇₂₋₈₄, Nef₁₂₆₋₁₄₄, Gp160₃₀₋₄₀, Gp160₄₁₋₅₃, Gp₃₀₈₋₃₂₃, and P24₈₋₁₅₁ in human and mice using immune-informatics analysis (Kardani et al. 2019; Khairkhah et al. 2018), we decided to design a multiepitope construct using novel epitopes derived from Rev protein. Herein, to predict highly conserved epitopes of Rev protein, we applied several immune-informatics web servers. Figure 1 indicates the workflow of *in silico* analysis.

Data acquisition and screening potential T-cell epitopes

At the first step of our study, the reference sequence of HIV-1 Rev protein was retrieved from HIV database (<https://www.hiv.lanl.gov/content/sequence/HIV/mainpage.html>). For prediction of peptide binding to mouse MHC molecules, the reference sequence of Rev protein was subjected to different web servers including SYFPEITHI (<http://www.syfpeithi.de/0-Home.htm>) using a support vector machine (SVM) multitask Kernel-based and IEDB MHC-I prediction tool (IEDB recommended method; <http://tools.iedb.org/mhci/>). Moreover, IEDB MHC-I prediction tool (IEDB recommended method) was applied (all predictions were done by default thresholds) to predict CTL epitopes for human MHC molecules (Khairkhah et al. 2018; Zhang et al. 2008). SYFPEITHI is a database containing T-cell epitopes, MHC-peptide motifs, and MHC ligands (Schuler et al. 2007). In addition, the analysis of TAP transport/proteasomal cleavage in order to predict antigen processing via the MHC I pathway was assessed by NetCTL 1.2 server at <http://www.cbs.dtu.dk/services/NetCTL/>. Prediction methods were achieved by default values (C-terminal cleavage, transport efficiency, and epitope identification were set on 0.15, 0.05, and 0.75, respectively).

Characterization of potential epitopes

Immunogenicity, allergenicity, and toxicity assessment

The predicted T-cell epitopes were further analyzed for immunogenicity, allergenicity, and toxicity prediction using IEDB immunogenicity predictor (<http://tools.iedb.org/immunogenicity/>) (default values) AlgPred (<https://webs.iiitd.edu.in/raghava/algpred/>) (Saha and

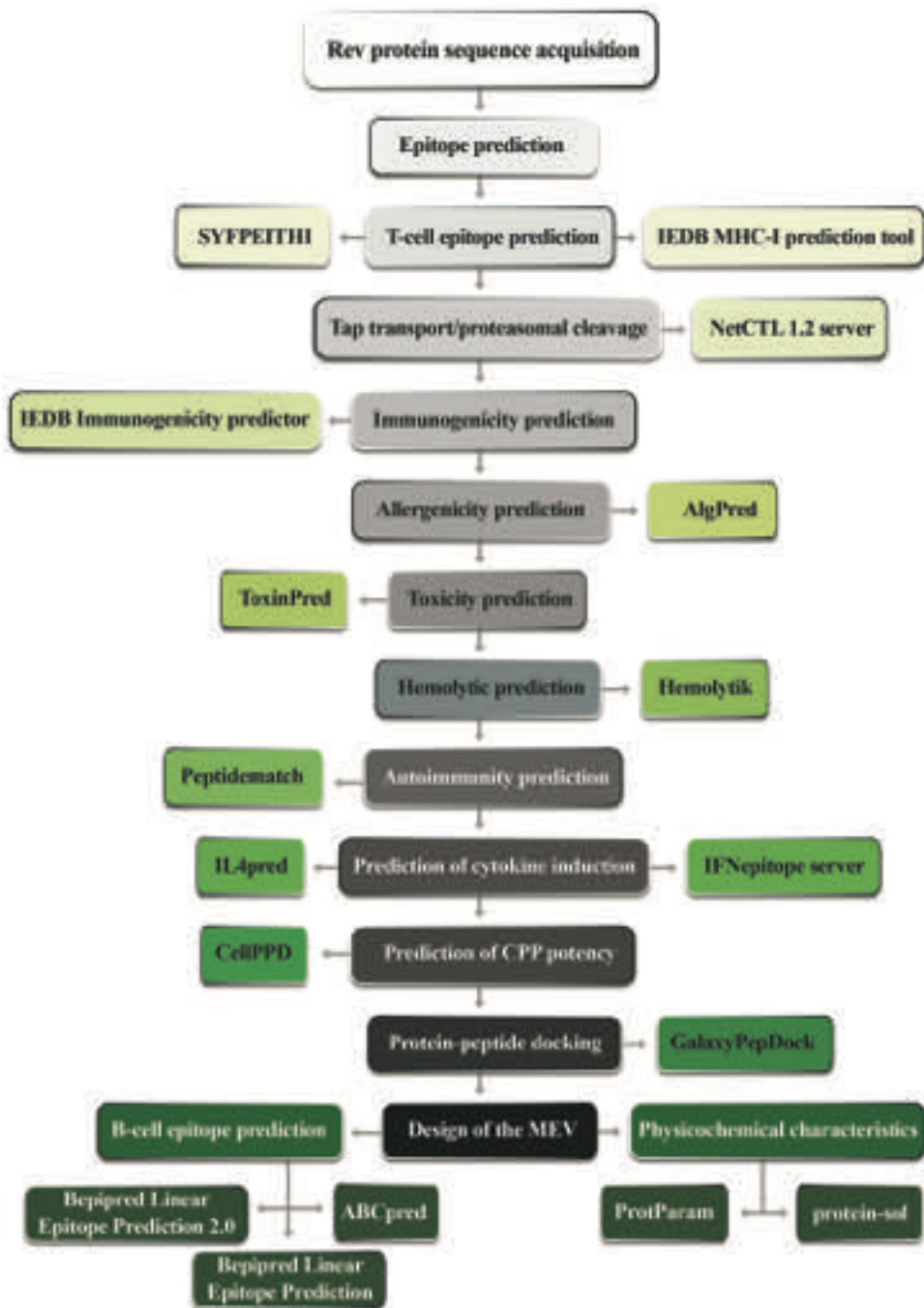


Figure 1. The total workflow of the *in silico* analysis.

Raghava 2006a) and ToxinPred (<https://webs.iitd.edu.in/raghava/toxinpred/>) (Gupta et al. 2013) tools, respectively. AlgPred predicts allergens from protein sequence. AlgPred server offers several approaches; (a) scanning IgE epitopes; (b) motif-based approach; (c) SVM-based method; (d) Hybrid approach; and (e) BLAST search on allergen representative

proteins (ARPs) (Saha and Raghava 2006a). ToxinPred can be useful in predicting (a) toxicity or non-toxicity of input peptides, (b) minimum mutations in peptides to increase or decrease their toxicity, and (c) toxic areas in proteins (Gupta et al. 2013).

Hemolytic and cross-reactivity prediction

The candidate epitopes were analyzed by peptide matching server using Apache Lucene-based search engine (<https://research.bioinformatics.udel.edu/peptidematch/index.jsp>) to evaluate the cross-reactivity between human proteome and peptides (Chen et al. 2013). Furthermore, to obtain the hemolytic potency of epitopes, the hemolytic web server (<https://webs.iiitd.edu.in/raghava/hemolytik/>) was applied (Gautam et al. 2014).

Prediction of cytokine induction

To assess the cytokine induction of candidate epitopes, we used IL4pred (<https://webs.iiitd.edu.in/raghava/il4pred/>) and IFNepitope (<https://webs.iiitd.edu.in/raghava/ifnepitope/>) web servers. One of the critical steps in vaccine design is determination of antigenic regions that activate T-helper cells. There are various types of T-helper cells including Th1, Th2, Th17, and each type of T-helper cells generates specific type of cytokines. For instance, IFN- γ was released by Th1 and eliminates intracellular pathogens. Thus, identification of IFN- γ inducing T-helper cells must be done to design an effective subunit vaccine (Dhanda et al. 2013b). The secretion of Interleukin-4 (IL4) is the characteristic of Th2 responses. IL4 has a critical function in antibody isotype switching and triggers the generation of IgE (Dhanda et al. 2013a).

Prediction of CPP potency

This prediction was added due to the regulatory role of Rev protein similar to Tat regulatory protein. It is possible for the existence of cell-penetrating peptides in Rev sequence. Thus, to assess the potential characteristic of epitopes to behave as a cell-penetrating peptide (CPP), the candidate epitopes were subjected to CellPPD web server at <https://webs.iiitd.edu.in/raghava/cellppd/> (Gautam et al. 2015).

Molecular interactions of CTL epitopes and HLA alleles

The GalaxyPepDock (<http://galaxy.seoklab.org/>) tool was used for *in silico* peptide-protein molecular docking studies of the candidate CTL epitopes with their respective human and mice HLA class I allele binders. There are three various algorithms to dock peptide-protein interaction including template-based docking, global docking, and local docking. The GalaxyPepDock webserver algorithm is template-based docking. The PDB files of MHC alleles were obtained from RCSB PDB server at <https://www.rcsb.org/>.

Design of a novel multi-epitope construct

A novel multi-epitope construct was designed using several CTL and HTL epitopes including Nef₆₀₋₇₁, Nef₇₂₋₈₄, Nef₁₂₆₋₁₄₄, Gp160₃₀₋₄₀, Gp160₄₁₋₅₃, Gp₃₀₈₋₃₂₃, and P24₈₋₁₅₁ as previously reported (Kardani et al. 2019; Khairkhan et al. 2018), as well as four CTL epitopes derived from Rev protein such as Rev₈₋₁₇, Rev₁₄₋₂₃, Rev₄₃₋₅₂ and Rev₅₃₋₆₃. Moreover, the alanine-alanine-tyrosine (AAY) was used as a flexible linker to optimize proteasome processing between the selected CTL and HTL epitopes. In order to start of the translation, the methionine residue (M) was placed at the N-terminal region. To purify and detect the

final product by anti-His tag antibody, the six histidine residues (6xHis) were placed at the C-terminal region. To induce strong immune responses, we designed a novel multiepitope construct comprising overlapping epitopes (7–24 amino acids in length); because it was confirmed that long peptides could generate more effective immune responses than short peptides (Kardani et al. 2019).

Characterization of the designed multiepitope construct

Screening potential B-cell epitopes

B-cell epitopes are the antigenic parts on the surface area of the targeted pathogens. After determination of B-cell epitopes by B-cell receptors (BCRs), induction of specific antibodies would occur. Thus, we used three different servers such as ABCpred (<https://webs.iitd.edu.in/raghava/abcpred/>) (Saha and Raghava 2006b), Bepipred Linear Epitope Prediction 2.0 (<http://tools.iedb.org/bcell/>), and Bepipred Linear Epitope Prediction (<http://tools.iedb.org/bcell/>) to predict B-cell epitopes in the full length of the designed multiepitope construct (all predictions were done by default thresholds) (Kardani et al. 2020).

Analysis of physicochemical characteristics

The ProtParam tool was used to predict the physicochemical characteristics of the designed multiepitope construct. The ProtParam tool calculates several physicochemical properties of the given protein sequence such as molecular weight, theoretical pI, half-life *in vitro/in vivo*, amino acid composition, instability index, aliphatic index, and grand average of hydropathicity (Gasteiger et al. 2005). In addition, to assess the protein solubility, the multiepitope construct was subjected to Protein-Sol webserver (<https://protein-sol.manchester.ac.uk/>) (Hebditch et al. 2017).

In vitro analysis

Preparation of the recombinant plasmids

The nucleotide sequence of the *nef-rev-gp160-p24* polyepitope DNA (named as *nef-rev-gp160-p24* gene) was obtained by amino acid reverse translation tool (http://www.bioinformatics.org/sms2/rev_trans.html), and synthesized in *Bam*HI/*Hind*III cloning site of pUC57 vector by Biomatik Company (Canada).

The recombinant eukaryotic expression vectors

To generate pcDNA-*nef-rev-gp160-p24* construct, the *nef-rev-gp160-p24* gene was subcloned from pUC57 into the pcDNA3.1 (-) expression vector (Invitrogen) in *Bam*HI/*Hind*III sites (Thermo Fisher Scientific) (Supplementary Figure 1). Also, to make pEGFP-*nef-rev-gp160-p24*, the *nef-rev-gp160-p24* gene was subcloned into *Xho*I/*Hind*III restriction site of the pEGFP-N1 expression vector (Clontech) using T4 DNA ligase (Fermentas, Germany) (Supplementary Figure 2). Finally, both eukaryotic expression vectors harboring the *nef-rev-gp160-p24* gene sequence were purified by Endo-free plasmid Mega kit (MN, Germany) and evaluated by NanoDrop spectrophotometer.

The recombinant prokaryotic expression vector

The pET-24a (+) prokaryotic expression vector (Novagen) was used to express the recombinant polypeptide. To construct pET-*nef-rev-gp160-p24*, the fragment was subcloned into the *Bam*HI/*Hind*III cloning sites of pET-24a (+) (Supplementary Figure 1).

Expression of the multiepitope polypeptide in bacteria

To express the recombinant multiepitope polypeptide, the pET-24a-*nef-rev-gp160-p24* was transformed into *E. coli* strains (BL21 and Rosetta). The kanamycin-resistant recombinant clones were selected on LB-agar (Sigma, Germany) and cultured in Ty2x medium to an OD₆₀₀ of 0.7–0.8. The expression of multiepitope polypeptide was induced by 1 mM Isopropyl thiogalactopyranoside (IPTG, Sigma) at 37°C. Incubation time (*i.e.*, 2, 4, 6 and 16 h) was optimized after induction. The cell pellets were harvested, and analyzed by 12.5% SDS-PAGE and western blot using anti-His tag antibody (Abcam, USA; 1:10000 v/v).

Purification of the multiepitope polypeptide

The purification of the recombinant (r) Nef-Rev-Gp160-P24 multiepitope polypeptide was performed by affinity chromatography using Ni-NTA agarose column (Macherey-Nagel) under denaturing conditions (containing 4 M urea, 20 mM Tris-HCl, 300 mM NaCl, 10 mM 2-Mercaptoethanol, 0.5% tween 20 and 1 M imidazole, pH = 7.9). Subsequently, the rNef-Rev-Gp160-P24 polypeptide was dialyzed against PBS 0.5X using a dialysis membrane (10 kDa). The final concentration and purity of the recombinant polypeptide were assessed by the Bradford kit and NanoDrop spectrophotometer. Moreover, the LAL assay (QCL-1000) was done to determine the contamination with LPS which was less than 0.5 EU/mg.

Preparation of the non-covalent DNA/CPPs and polypeptide/CPPs nanoparticles

MPG (GALFLGFLGAAGSTMGAWSQPKKRKRKV), HR9 (CHHHHRRRRRRRRRRHHH HHC), CyLoP-1 (CRWRWKCKK) and LDP-NLS (KWRRKLLKLRPKKKRKRKV) peptides were synthesized by Biomatik Corporation (Canada). To form CPP/DNA complexes including MPG/pEGFP-N1-*nef-rev-gp160-p24*, HR9/pEGFP-N1-*nef-rev-gp160-p24*, MPG/pcDNA3.1-*nef-rev-gp160-p24* and HR9/pcDNA3.1-*nef-rev-gp160-p24* complexes, 2 µg of pEGFP-N1-*nef-vpr-gp160-p24* and pcDNA3.1-*nef-rev-gp160-p24* were mixed with MPG and HR9 at certain nitrogen to phosphate ratios (N/P) of 10 and 5, respectively, and incubated at room temperature for 1 hr (Namazi et al. 2019). The formation of different complexes (nanoparticles) was confirmed using gel retardation assay, Zetasizer (Malvern Instruments) and scanning electron microscope (FEI Quanta 200 SEM). To form the CPP/polypeptide complexes including CyLoP-1/rNef-Rev-Gp160-P24 and LDP-NLS/rNef-Rev-Gp160-P24 complexes, 2 µg of the polypeptide was mixed with the CyLoP-1 and LDP-NLS CPPs at certain molar ratio of 1:10 (polypeptide: CPP) and incubated at room temperature for 60 min (Namazi et al. 2019). The formation of different complexes was confirmed by SEM and Zetasizer indicating morphology, size, and charge of nanoparticles.

Transfection of HEK-293 T cells with the CPP/DNA nanoparticles

The 5×10^4 HEK-293 T cells/well pre-cultured in complete DMEM (Gibco, Germany) containing 10% heat-inactivated FBS (Gibco) at 37°C and 5% CO₂, were seeded in a 24-well plate (Greiner) for 24 hrs. The MPG or HR9/pEGFP-N1-*nef-rev-gp160-p24* nanoparticles

were prepared at the N/P ratios of 10 and 5, respectively, added to cells, and incubated at 37°C for 48 hrs. The transfection efficiency was assessed by Fluorescence microscope and Flow cytometry (Partec). Additionally, TurboFect (Fermentas, Germany)/pEGFP-N1 and TurboFect/pEGFP-N1-*nef-rev-gp160-p24* complexes were applied as a positive control, while the untreated cells were used as a negative control.

In vivo analysis

Mice immunization

Six to eight-week-old inbred female BALB/c mice (4 per group) were obtained from the Department of Animal Science at Pasteur Institute of Iran. All mice were housed under specific pathogen-free conditions and allowed to adapt to new conditions one week before the experiment based on the guidelines of Pasteur Institute of Iran for scientific purposes. Fifteen mouse groups divided randomly were immunized subcutaneously at the footpad with different modalities as shown in Table 1. Mice were immunized on days 0, 14, and 28 with 50 µg of the naked DNA, the DNA (5 µg)/HR9 nanoparticles (N:P = 5), the DNA (5 µg)/MPG nanoparticles (N:P = 10), the recombinant polypeptide (5 µg) emulsified in Montanide adjuvant at ratio of 30:70 v/v, and the recombinant polypeptide (5 µg)/CyLop-1 or LDP-NLS nanoparticles (molar ratio = 1:10 for polypeptide: CPP).

Evaluation of antibody responses

To determine humoral immune response against rNef-Rev-Gp160-P24 antigen (5 µg/mL), the pooled sera were prepared from each group four weeks after the third injection. The levels of anti-rNef-Rev-Gp160-P24 total IgG (Sigma; 1:10000 v/v) and its subclasses including IgG1, IgG2a, and IgG2b (Sigma; 1:10000 v/v) were evaluated in the sera using indirect ELISA. Tetramethylbenzidine (TMB) was used as a substrate.

Cytokine assay

To evaluate cellular immune response, four weeks after the third immunization, all mice from each group were sacrificed and the spleens were detached. The red blood cells were lysed and 2×10^6 cells/mL of pooled splenocytes were cultured in 96-well plates for 72 hr in complete RPMI-1640 culture medium supplemented by 5% FBS. All samples from each group were treated with rNef-Rev-Gp160-P24 polypeptide (5 µg/mL), concanavalin A (5 µg/mL, positive control) and RPMI 5% (negative control) in triplicates. The presence of IFN-γ, IL-10 and IL-5 in supernatants was assessed by a sandwich-based ELISA system (Mabtech Co.).

In vitro CTL activity

The *in vitro* CTL activity was measured by Granzyme B (GrB) ELISA assay. To reach this aim, 2×10^4 cells/well of P815 as target cells (T) were seeded triplicate in 96-well plates and treated with rNef-Rev-Gp160-P24 antigen (30 µg/mL) for 24 hr. The splenocytes were used as effector cells (E). To observe the maximal release of Granzyme B, the effector cells were added to the target cells at ratio of 100:1 and cocultured in RPMI-1640 10% for 6 hr. Then, the supernatants were harvested, and Granzyme B concentrations were evaluated by ELISA (eBioscience).

Table 1. Mice immunization program.

Group	Modality	First injection (Day 0)	Second injection (Day 14)	Third injection (Day 28)
G1	DNA/DNA/DNA	pcDNA _{nef-rev-gp160-p24}	pcDNA _{nef-rev-gp160-p24}	pcDNA _{nef-rev-gp160-p24}
G2	DNA/DNA/DNA	pcDNA _{nef-rev-gp160-p24} + MPG	pcDNA _{nef-rev-gp160-p24} + MPG	pcDNA _{nef-rev-gp160-p24} + MPG
G3	DNA/DNA/DNA	pcDNA _{nef-rev-gp160-p24} + HR9	pcDNA _{nef-rev-gp160-p24} + HR9	pcDNA _{nef-rev-gp160-p24} + HR9
G4	Polypeptide/Polypeptide/Polypeptide	rNef-Rev-Gp160-P24 + Montanide	rNef-Rev-Gp160-P24 + Montanide	rNef-Rev-Gp160-P24 + Montanide
G5	Polypeptide/Polypeptide/Polypeptide	rNef-Rev-Gp160-P24 + CyLoP-1	rNef-Rev-Gp160-P24 + CyLoP-1	rNef-Rev-Gp160-P24 + CyLoP-1
G6	Polypeptide/Polypeptide/Polypeptide	rNef-Rev-Gp160-P24 + LDP-NLS	rNef-Rev-Gp160-P24 + LDP-NLS	rNef-Rev-Gp160-P24 + LDP-NLS
G7	DNA/Polypeptide/Polypeptide	pcDNA _{nef-rev-gp160-p24} + MPG	rNef-Rev-Gp160-P24 + Montanide	rNef-Rev-Gp160-P24 + Montanide
G8	DNA/Polypeptide/Polypeptide	pcDNA _{nef-rev-gp160-p24} + MPG	rNef-Rev-Gp160-P24 + CyLoP-1	rNef-Rev-Gp160-P24 + CyLoP-1
G9	DNA/Polypeptide/Polypeptide	pcDNA _{nef-rev-gp160-p24} + MPG	rNef-Rev-Gp160-P24 + LDP-NLS	rNef-Rev-Gp160-P24 + LDP-NLS
G10	DNA/Polypeptide/Polypeptide	pcDNA _{nef-rev-gp160-p24} + HR9	rNef-Rev-Gp160-P24 + Montanide	rNef-Rev-Gp160-P24 + Montanide
G11	DNA/Polypeptide/Polypeptide	pcDNA _{nef-rev-gp160-p24} + HR9	rNef-Rev-Gp160-P24 + CyLoP-1	rNef-Rev-Gp160-P24 + CyLoP-1
G12	DNA/Polypeptide/Polypeptide	pcDNA _{nef-rev-gp160-p24} + HR9	rNef-Rev-Gp160-P24 + LDP-NLS	rNef-Rev-Gp160-P24 + LDP-NLS
G13	Control	CyLoP-1	CyLoP-1	CyLoP-1
G14	Control	LDP-NLS	LDP-NLS	LDP-NLS
G15	Control	PBS	PBS	PBS

pcDNA_{nef-rev-gp160-p24}: pcDNA3.1 (-) containing the *nef-rev-gp160-p24* gene; rNef-Rev-Gp160-P24: recombinant Nef-Rev-Gp160-P24 polypeptide

Statistical analysis

Prism 5.0 software (GraphPad) was applied for statistical analysis. The differences between the groups were determined by one-way ANOVA (GraphPad Software). The results were shown as mean (as column) \pm standard deviation (SD as bar) for each group. The $p < .05$ was statistically considered significant (* $p < .05$, ** $p < .01$ and *** $p < .001$). The studies were performed in two independent experiments.

Results

In silico analysis

Screening potential epitopes

We identified four CTL epitopes in the Rev protein corresponding to MHC molecule class I supertype representative using SYFPEITHI and IEDB MHC-I prediction tools for mouse MHC alleles in pre-clinical evaluation and IEDB MHC-I prediction tool for human alleles (Table 2). In addition, to predict TAP transport efficiency and proteasomal C-terminal cleavage scores of Rev-derived epitopes, the NetCTL 1.2 webserver was used. The selected epitopes had the highest prediction scores (Table 3).

Characterization of potential epitopes

The toxicity and allergenicity of the candidate epitopes were evaluated using ToxinPred and AlgPred web servers. The results indicated that the selected epitopes were no toxic and no allergenic. Also, we investigated immunogenicity prediction by IEDB immunogenicity predictor, and the results showed that the selected epitopes had the highest immunogenicity scores. Moreover, the hemolytic and non-hemolytic activities of the peptide sequences were analyzed, and the ranges were between 0 (non-hemolytic) and 1 (hemolytic). The results indicated that the selected epitopes are in the middle of this range (0.49). Furthermore, the outcomes of the cross-reactivity assessment using peptide matching server determined that there was no cross-reactivity between human proteome and peptides. The prediction of cytokine induction (IL4 and IFN- γ) showed that all of the four candidate epitopes are cytokine inducers. Moreover, the CPP potency of the epitopes was investigated by CellPPD tool and one of the epitopes (Rev₄₃₋₅₂) was recognized as a CPP with +4.00 net charge (Table 3).

Molecular interactions of CTL epitopes and HLA alleles

One of *in silico* critical steps to design vaccines is peptide-protein molecular docking. Predicting the binding site of a ligand and a receptor, and the peptide-protein interaction is the original aim of computational docking (Sahni and Nagendra 2004). Herein, to assess the interaction similarity between candidate epitopes and both human and mice HLA alleles, a docking webserver (GalaxyPepDock) based on template-based docking algorithm, was utilized. Its results were indicated in Table 4. Also, the highest interaction similarity scores and some examples of protein-peptide molecular docking have been illustrated in Figure 2.

Design of a novel multiepitope construct

The designed non-toxic and non-allergenic multiepitope construct with high scores of CTL and HTL immunogenic epitopes linked by AAY sequence have been illustrated in Figure 3.

Table 2. Prediction of CTL epitopes.

Epitope	Human allele	SYFPEITHI score	Mouse allele	SYFPEITHI score	Mouse allele	IEDB score	
Rev ₈₋₁₇	HLA-A*02:01	20	H2-Db	11	H-2-Kk	0.85	
	HLA-B*15:16	16	H2-Kd	13	H-2-Kb	0.017	
	HLA-B*13	13	H2-Kk	19	H-2-Dd	0.016	
	HLA-B*37	16			H-2-Ld	0.011	
	HLA-B*39:01	12					
	HLA-B*47:01	19					
	HLA-B*49:01	13					
	HLA-B*51:01	14					
HLA-A*01	10						
Rev ₁₄₋₂₃	HLA-A*01	19	H2-Kb	10	H-2-Kb	0.264	
	HLA-A*03	23	H2-Kk	5	H-2-Kk	0.013	
	HLA-A*11:01	16			H-2-Dd	0.012	
	HLA-A*26	24					
	HLA-A*68:01	10					
	HLA-B*14:02	11					
	HLA-B*15:01	21					
	HLA-B*58:02	18					
	HLA-B*53:01	11					
	HLA-B*44:02	14					
	HLA-B*35:01	13					
	HLA-B*27:05	12					
Rev ₄₃₋₅₂	HLA-B*13	14	H2-Db	10	H-2-Kd	0.135	
	HLA-B*27:05	23	H2-Kd	11	H-2-Kb	0.105	
	HLA-B*38:01	12	H2-Kk	11	H-2-Dd	0.04	
	HLA-B*39:01	16	H2-Ld	6	H-2-Kk	0.02	
	HLA-A*03	13			H-2-Db	0.013	
	HLA-B*08	22			H-2-Ld	0.012	
	HLA-B*15:16	14					
	HLA-B*27:09	15					
	HLA-B*49:01	12					
	HLA-B*51:01	13					
	HLA-B*58:02	19					
	Rev ₅₃₋₆₃	HLA-A*01	27	H2-Ld	10	H-2-Kk	0.116
		HLA-A*02:01	22	H2-Kb	13	H-2-Kb	0.076
HLA-A*03		21	H2-Kk	14	H-2-Dd	0.0184	
HLA-A*11:01		17					
HLA-A*26		23					
HLA-B*08		16					
HLA-B*15:01		14					
HLA-B*18		22					
HLA-B*35:01		13					
HLA-B*44:02		14					
HLA-B*53:01		13					
HLA-B*58:02		13					

Characterization of the designed multiepitope construct

Screening potential B-cell epitopes

The full length of the novel multiepitope construct was subjected to three different web-servers to identify the potential B-cell epitopes. Various regions of the multiepitope construct were determined as B-cell epitopes (Figure 4). In addition, Table 5 shows the positions and the sequences of the identified B-cell epitopes.

Table 3. Characteristics of the potential CTL epitopes.

Epitope	Proteasomal C-terminal cleavage Score	Tap Transport Efficiency	Toxicity	Allergenicity	Immunogenicity	Hemolytic Probability	CPP Prediction	Charge	IL4 inducer prediction	IFN- γ epitope prediction
Rev ₈₋₁₇	0.8695	-0.0860	Non-toxin	Non-allergen	0.31409	0.49*	Non-CPP	-2.00	IL4-inducer	Positive
Rev ₁₄	0.9578	3.0890	Non-toxin	Non-allergen	-0.0836	0.48	Non-CPP	+2.00	IL4-inducer	Positive
Rev _{43-²³}	0.4948	1.2060	Non-toxin	Non-allergen	0.13884	0.49	CPP	+4.00	IL4-inducer	Positive
Rev _{53-⁵²}	0.9605	2.8980	Non-toxin	Non-allergen	0.19507	0.49	Non-CPP	+0.50	IL4-inducer	Positive
Rev ₆₃										

* Ranges were between 0 and 1, i.e. 1 very likely to be hemolytic, 0 very unlikely to be hemolytic.

Table 4. Peptide-protein interaction similarity scores between the selected CTL epitopes and MHC alleles of human and mice using Galaxy PepDock tool (<http://galaxy.seoklab.org/>).

HLA alleles	GalaxyPepDock			
	REV ₈₋₁₇	REV ₁₄₋₂₃	REV ₄₃₋₅₂	REV ₅₃₋₆₃
HLA A0301	157.0	211.0	175.0	196.0
HLA A1101	144.0	214.0	172.0	199.0
HLA A2402	175.0	175.0	192.0	186.0
HLA A3401	140.0	214.0	166.0	195.0
HLA A6801	156.0	214.0	178.0	190.0
HLA A7401	163.0	217.0	187.0	196.0
HLA B1301	174.0	241.0	168.0	221.0
HLA B3901	147.0	231.0	150.0	217.0
HLA B4101	163.0	230.0	159.0	213.0
HLA B5601	162.0	248.0	164.0	221.0
HLA B7301	157.0	221.0	165.0	188.0
H-2-Kb	157.0	201.0	201.0	188.0
H-2-Kd	204.0	183.0	185.0	194.0
H-2-Dd	158.0	179.0	165.0	193.0
H-2-Db	229.0	188.0	195.0	186.0
H-2-Ld	297.0	245.0	266.0	252.0

Physicochemical properties

Herein, the physicochemical properties of the designed multiepitope construct were investigated by ProtParam tool, and were given the Molecular weight (MW.) of 32.859 KDa and theoretical isoelectric point (pI) of 9.08. The instability index was 42.87, thus the polypeptide was classified as an unstable protein (an instability index <40 shows a stable protein/polypeptide). Also, the grand average of hydropathicity (GRAVY) was computed as -0.244 and the aliphatic index was 83.45%. Furthermore, the half-life was estimated 30 hrs for reticulocytes, more than 20 hrs for yeast, and more than 10 hrs for *E. coli*. Finally, the extinction coefficient (with/without Cys; $M^{-1} \text{ cm}^{-1}$ at 280 nm in water) was calculated as 67965/67840 (Table 6). Additionally, in order to calculate the protein solubility of the multiepitope construct, Protein-Sol webserver was used. The predicted scaled solubility was 0.231 and indicated the less solubility of the multiepitope construct (the predicted values lower than scaled solubility value which is 0.45 are predicted as a less soluble protein, and in contrast, any protein with greater scaled solubility value is predicted as higher solubility).

In vitro analysis

Subcloning of the *nef-rev-gp160-p24* gene in different vectors

The *nef-rev-gp160-p24* gene was successfully subcloned into pET-24a (+) as prokaryotic expression vector and pEGFP-N1 and pcDNA3.1 (-) as eukaryotic vectors. The *nef-rev-gp160-p24* gene was detected as a clear band of ~870 bp after digestion on agarose gel (data not shown) and confirmed by sequencing (Sanger sequencing method; 100% similarity with the designed gene construct).

Generation of the recombinant polypeptide

The higher yield of rNef-Rev-Gp160-P24 polypeptide expression was detected in Rosetta strain at 37°C and 4-h post-induction. The recombinant polypeptide was successfully

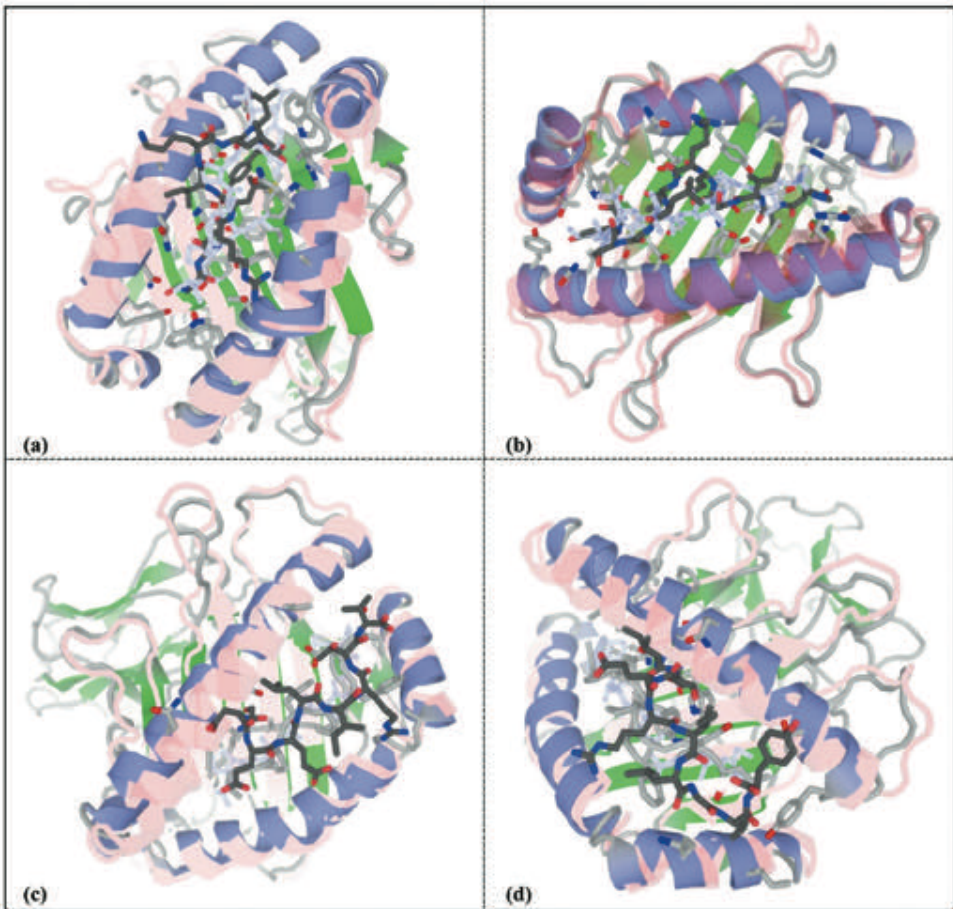


Figure 2. The examples of peptide-protein molecular docking: Successful peptide-protein docking between REV₁₄₋₂₃ and HLA A6801 with interaction score of 214.0 (a); Successful peptide-protein docking between REV₅₃₋₆₃ and HLA B5601 with interaction score of 221.0 (b); Successful peptide-protein docking between REV₈₋₁₇ and H-2-Ld with interaction score of 297.0 (c), Successful peptide-protein docking between REV₅₃₋₆₃ and H-2-Ld with interaction score of 252.0 (d).

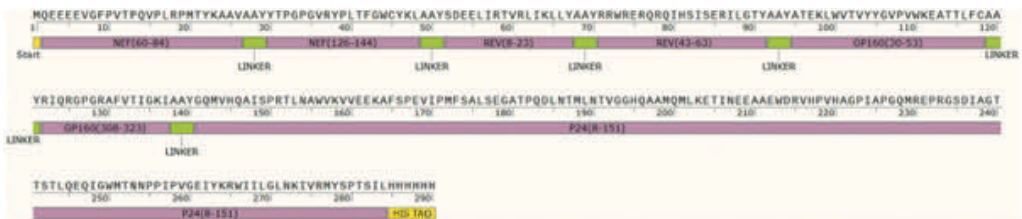


Figure 3. The schematic presentation of the designed multi-epitope peptide construct.

purified under denaturing conditions and observed as a ~ 35 kDa band in SDS-PAGE and western blotting (Figure 5).

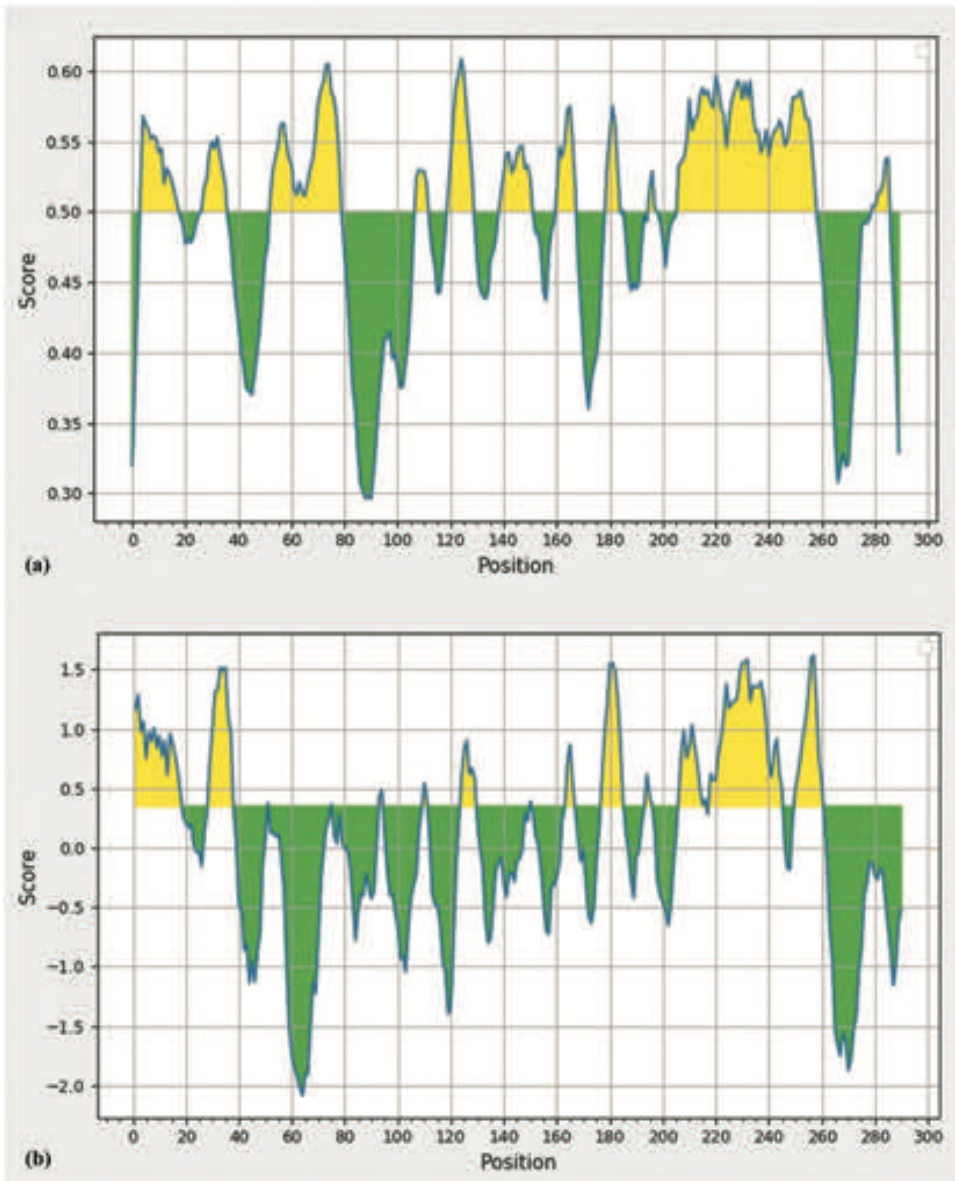


Figure 4. Linear B-cell epitopes prediction of the multiepitope construct using BepiPred 2.0 (a), and BepiPred (b). The residues with higher scores than the threshold were predicted to be part of an epitope as indicated in yellow color.

Characterization of the nanoparticles

The interaction between MPG/HR9 peptide and the recombinant DNA plasmids harboring Nef-Rev-Gp160-P24 coding sequence (pEGFP-N1-*nef-rev-gp160-p24* or pcDNA3.1-*nef-rev-gp160-p24*) was analyzed by gel retardation assay. For this aim, the recombinant vectors were mixed with MPG and HR9 at certain N/P ratios of 10 and 5, respectively. The results indicated that DNA did not migrate on agarose gel at certain N/P ratios confirming the formation of CPP/DNA complexes (Figure 6). On the other hand, the pEGFP-N1-*nef-rev-gp160-p24*

Table 5. Predicted B-cell epitopes of the designed multiepitope construct using several webservers.

Sequence			
No.	Bepired Linear Epitope Prediction 2.0	Position	Length
1	EEEVGFVPTPQVPLR	4–18	15
2	PVWKE	108–112	5
3	YGQMVHQAIISPR	140–151	12
4	EEKAFSPE	161–168	8
5	ATPQD	180–184	5
6	N	186	1
7	QAAM	196–199	4
8	NEEAAEWDRVHPVHAGPIAPGQMREPRGSDIAGTTSTLQEQIGWMTNPPPIV	207–259	53
Bepired Linear Epitope Prediction			
1	MQEEEEVGFVPTPQVPLR	1–18	18
2	Y	51	1
3	E	75	1
4	WK	110–111	2
5	QRGPGR	124–129	6
6	P	150	1
7	AFS	164–166	3
8	SEGATPQDL	177–185	9
9	GHQ	194–196	3
10	INEEAAEWDRV	206–216	11
11	PVHAGPIAPGQMREPRGSDIAGTTSTLQ	218–245	28
12	WMTNPPPIVG	250–260	11
ABCpred			
Rank	Sequence	Start Position	Score*
1	GPGVRYPLTFGWCYKL	33	0.93
1	HAGPIAPGQMREPRGS	220	0.93
2	PVGEIYKRWILGLNK	258	0.91
2	LSEGATPQDLNMLNT	176	0.91
3	WVTVYYGVPVWKEATT	100	0.90
4	GQMREPRGSDIAGTTS	227	0.89
5	EEEVGFVPTPQVPLRP	4	0.87
6	EAAEWDRVHPVHAGP	208	0.86
6	PEVIPMFSALSEGATP	167	0.86
7	AAMQMLKETINEEAAE	197	0.83
8	TSTLQEQIGWMTNPP	241	0.81
9	VHQAIISPRTLNAWVKV	144	0.80
10	YRRWRERQRQIHSISE	70	0.79
11	GWMTNPPPIVGEIYK	249	0.75
12	PRTLNAWVKVVEEKAF	150	0.74
13	YATEKLWVTVYYGVPV	94	0.72
13	RWILGLNKIVRMYS	265	0.72
13	PVTPQVPLRPMYKAA	10	0.72
14	LNTVGGHQAAMQMLKE	189	0.67
15	DEELIRTVRLIKLLYA	53	0.64
15	WVKVVEEKAFSPEVIP	156	0.64
16	QDLNMLNTVGGHQAA	183	0.56

* Higher score of the peptide means the higher probability to be as epitope; All the peptides shown here are above the threshold value chosen.

(−20.2 mV), pcDNA3.1 (−)-*nef-rev-gp160-p24* (−24.1 mV) and rNef-Rev-Gp160-P24 (−24.3 mV) had negative charges at 25°C, while the MPG/pEGFP-N1-*nef-rev-gp160-p24* (+24.8 mV), MPG/pcDNA3.1-*nef-rev-gp160-p24* (+25.21 mV), HR9/pEGFP-N1-*nef-rev-gp160-p24* (+22.8 mV), HR9/pcDNA3.1-*nef-rev-gp160-p24* (+23.7 mV), CyLoP-1/rNef-Rev-Gp160-P24 (+4.05 mV), and LDP-NLS/rNef-Rev-Gp160-P24 (+4.01 mV) nanoparticles had positive charges. Moreover, the spherical MPG/pEGFP-N1-*nef-rev-gp160-p24* nanoparticles

Table 6. The physicochemical features of the designed multi-epitope construct.

Sequence	Negatively charged residues (Asp + Glu)	Positively charged residues (Arg + Lys)	Number of aa ¹	MW ² (kDa)	pI ³	Extinction coefficient (with/without Cys) ⁴	Half-life ⁵	Instability index	Aliphatic index ⁶	Grand average of hydropathicity	Solubility
rNef-Rev-Gp160-P24	25	30	290	32.859	9.08	67965/67840	30 hr, >20 hr, and >10 hr	42.87	83.45	-0.244	0.231 (Less soluble)

¹aa: amino acid.²MW: molecular weight.³pI: isoelectric point.⁴Extinction coefficients are in units of $M^{-1} \text{ cm}^{-1}$, at 280 nm measured in water.⁵mammalian reticulocytes (*in vitro*), yeast (*in vivo*), and *E. coli* (*in vivo*), respectively⁶A protein with instability index smaller than 40 is categorized as stable.

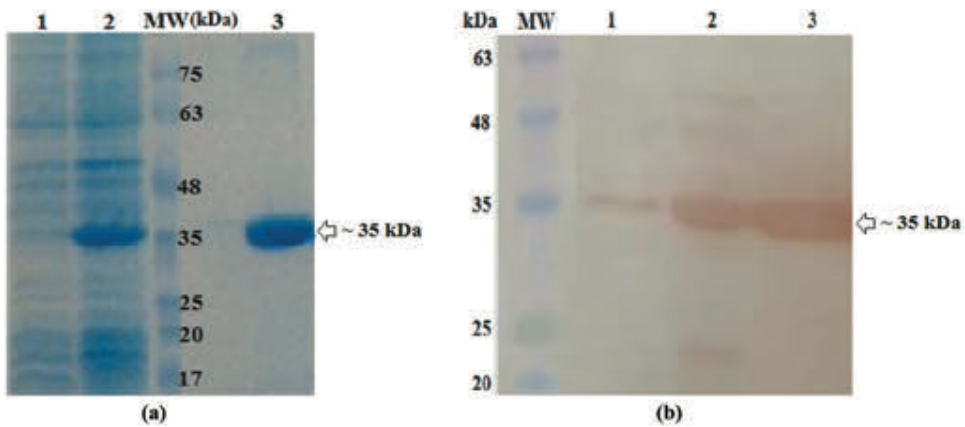


Figure 5. Analysis of expression and purification of the rNef-Rev-Gp160-P24 polypeptide in Rosetta using SDS-PAGE (a) and western blotting (b): Lane 1: before induction in Rosetta containing pET-24a (+)-*nef-rev-gp160-p24*, Lane 2: 4 h after induction in Rosetta containing pET-24a (+)-*nef-rev-gp160-p24*, Lane 3: the purified rNef-Rev-Gp160-P24 polypeptide. MW: Molecular weight marker (prestained protein ladder, 10–180 kDa, Fermentas).

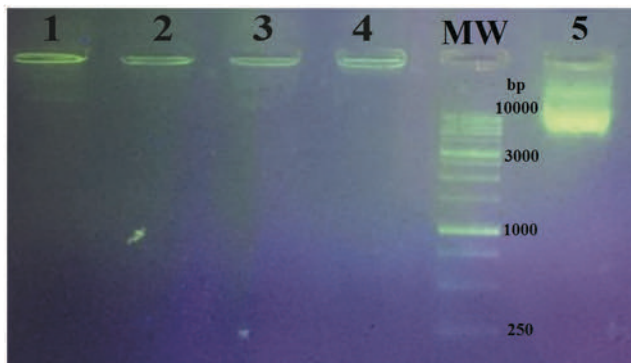


Figure 6. Gel retardation assay of the CPPs/DNA complexes. Lane 1: The MPG/pEGFP-*nef-rev-gp160-p24* complexes at N/P ratio of 10, Lane 2: The MPG/pcDNA-*nef-rev-gp160-p24* complexes at N/P ratio of 10, Lane 3: The HR9/pEGFP-*nef-rev-gp160-p24* complexes at N/P ratio of 5, Lane 4: The HR9/pcDNA-*nef-rev-gp160-p24* complexes at N/P ratio of 5, Lane 5: the naked pcDNA-*nef-rev-gp160-p24* as a control. MW (Molecular size marker, 1 kb, Fermentas).

showed an average size of ~ 150–200 nm, whereas the non-spherical HR9/pEGFP-N1-*nef-rev-gp160-p24* nanoparticles indicated an average size of ~ 100–200 nm. The spherical CyLoP-1/rNef-Rev-Gp160-P24 nanoparticles showed an average size of ~ 200–350 nm, whereas the non-spherical LDP-NLS/rNef-Rev-Gp160-P24 nanoparticles indicated an average size of ~ 100–200 nm (Table 7).

In vitro delivery of the CPP/DNA nanoparticles into the cell

The potency of HR9 and MPG CPPs for delivery of pEGFP-N1-*nef-rev-gp160-p24* into HEK-293 T mammalian cells at the certain N/P ratios of 5 and 10, respectively, was evaluated at 48 hr after transfection. The results showed that no measurable fluorescence was detected in the

Table 7. Zeta potential, size and morphology of different types of nanoparticles.

Carrier/Cargo	Nanoparticles	Zeta Potential (mV)	Size (nm)	Shape of Complexes
CPP/polypeptide	LDP-NLS/rNef-Rev-Gp160-P24	+4.01	~ 100–200	Non-spherical
	CyLoP-1/rNef-Rev-Gp160-P24	+4.05	~ 200–350	Spherical
CPP/DNA	MPG/pEGFP-N1- <i>nef-rev-gp160-p24</i>	+24.8	~ 150–200	Spherical
	HR9/pEGFP-N1- <i>nef-rev-gp160-p24</i>	+22.8	~ 100–200	Non-spherical
	MPG/pcDNA3.1 (-)- <i>nef-rev-gp160-p24</i>	+25.21	~ 100–150	Spherical
	HR9/pcDNA3.1 (-)- <i>nef-rev-gp160-p24</i>	+23.7	~ 100–150	Non-spherical
Controls	rNef-Rev-Gp160-P24	-24.3	~ 150–300	-
	pEGFP-N1- <i>nef-rev-gp160-p24</i>	-20.2	~ 100–200	-
	pcDNA3.1 (-)- <i>nef-rev-gp160-p24</i>	-24.1	~ 100–150	-

untransfected cells incubated with the naked DNA. The cellular uptake of TurboFect/pEGFP-N1, TurboFect/pEGFP-N1-*nef-rev-gp160-p24*, MPG/pEGFP-N1-*nef-rev-gp160-p24* and HR9/pEGFP-N1-*nef-rev-gp160-p24* complexes were $85.09\% \pm 2.80$, $49.02\% \pm 1.88$, $39.11\% \pm 0.67$ and $28.08\% \pm 0.42$, respectively (Table 8). *In vitro* assessment indicated a significant difference in DNA delivery using HR9 and MPG peptides ($p < .05$).

In vivo analysis

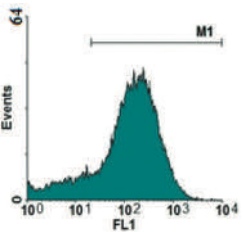
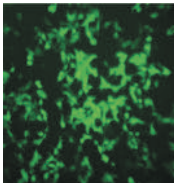
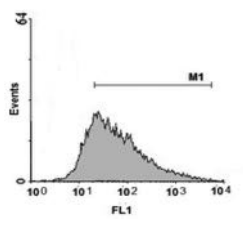
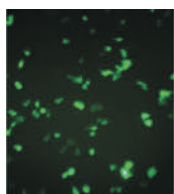
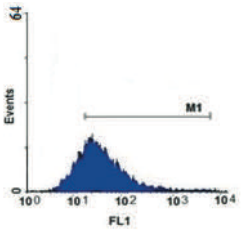
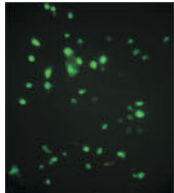
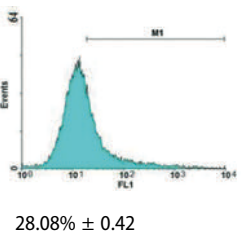
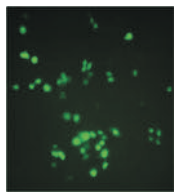
Measurement of antibody responses

The levels of total IgG and its subclasses in sera of mice were evaluated four weeks after the third immunization. A significant difference was detected in the levels of total IgG and its subclasses between groups that received different vaccine formulations (G1-G12) and controls (G13-G15) ($p < .05$, Figure 7). Moreover, the significant differences were observed at the levels of total IgG, IgG2a and IgG2b between groups that received the naked DNA (G1) and homologous DNA/MPG or DNA/HR9 nanoparticles (G2 and G3) ($p < .05$, Figure 7). Interestingly, no significant differences at the levels of total IgG and isotypes were observed between groups injected with homologous DNA/MPG nanoparticles (G2) and groups injected with homologous DNA/HR9 nanoparticles (G3, $p > .05$, Figure 7). The highest level of total IgG was observed in groups receiving homologous rNef-Rev-Gp160-P24 polypeptide along with Montanide or CPPs (G4-G6). The group immunized with the homologous rNef-Rev-Gp160-P24 polypeptide + Montanide (G4) showed the highest level of IgG1 in comparison with other groups. All heterologous DNA prime/polypeptide boost regimens elicited more effective anti-rNef-Rev-Gp160-P24-specific IgG2a and IgG2b antibody responses than other groups in mice (G7-G12, $p < .001$, Figure 7). Indeed, the ratios of mean IgG2a/IgG1 and IgG2b/IgG1 were higher in mice receiving these regimens compared to other groups suggesting Th1 immune response.

Cytokine secretion

The results of IL-5, IL-10 and IFN- γ secretion indicated that all mice immunizations with different modalities could efficiently increase the secretion of IFN- γ cytokine compared to controls ($p < .05$, Figure 8a). Additionally, the highest levels of IFN- γ secretion were detected in mice immunized with heterologous DNA+MPG or HR9 prime/polypeptide +LDP-NLS boost (G9 and G12) regimens compared to other groups ($p < .01$). The DNA delivered by MPG or HR9 was more potent than the naked DNA for inducing IFN- γ cytokine ($p < .001$, Figure 8a). There was no significant difference between the levels of rNef-Rev-Gp160-P24-specific IL-5 secretion in various formulations using HR9, MPG,

Table 8. DNA delivery using MPG and HR9 CPPs into HEK-293 T cells.

Groups	Flow Cytometry Results (%)*	Fluorescent Microscopy Results
TurboFect/pEGFP-N1		
TurboFect/pEGFP-N1- <i>nef-rev-gp-p24</i>	85.09% ± 2.80 	
MPG/pEGFP-N1- <i>nef-rev-gp-p24</i>	49.02% ± 1.88 	
HR9/pEGFP-N1- <i>nef-rev-gp-p24</i>	39.11% ± 0.67 	
	28.08% ± 0.42	

* The study was performed in two independent experiments and in duplicate for each sample.

LDP-NLS and CyLoP-1 ($p > .05$, [Figure 8b](#)). The lowest levels of IL-10 were importantly observed in mice receiving rNef-Rev-Gp160-P24 polypeptide in homologous (G6) or heterologous (G9 and G12) regimens delivered by LDP-NLS CPP ($p < .05$, [Figure 8c](#)). The ratios of mean IFN- γ /IL-10 and IFN- γ /IL-5 for all test groups were considerably more than controls (G13-G15; $p < .05$; [Figure 8](#)).

Evaluation of Granzyme B

For *in vitro* CTL activity, the Granzyme B secretion was assessed four weeks after the third immunization. Higher levels of Granzyme B were observed in groups immunized with the

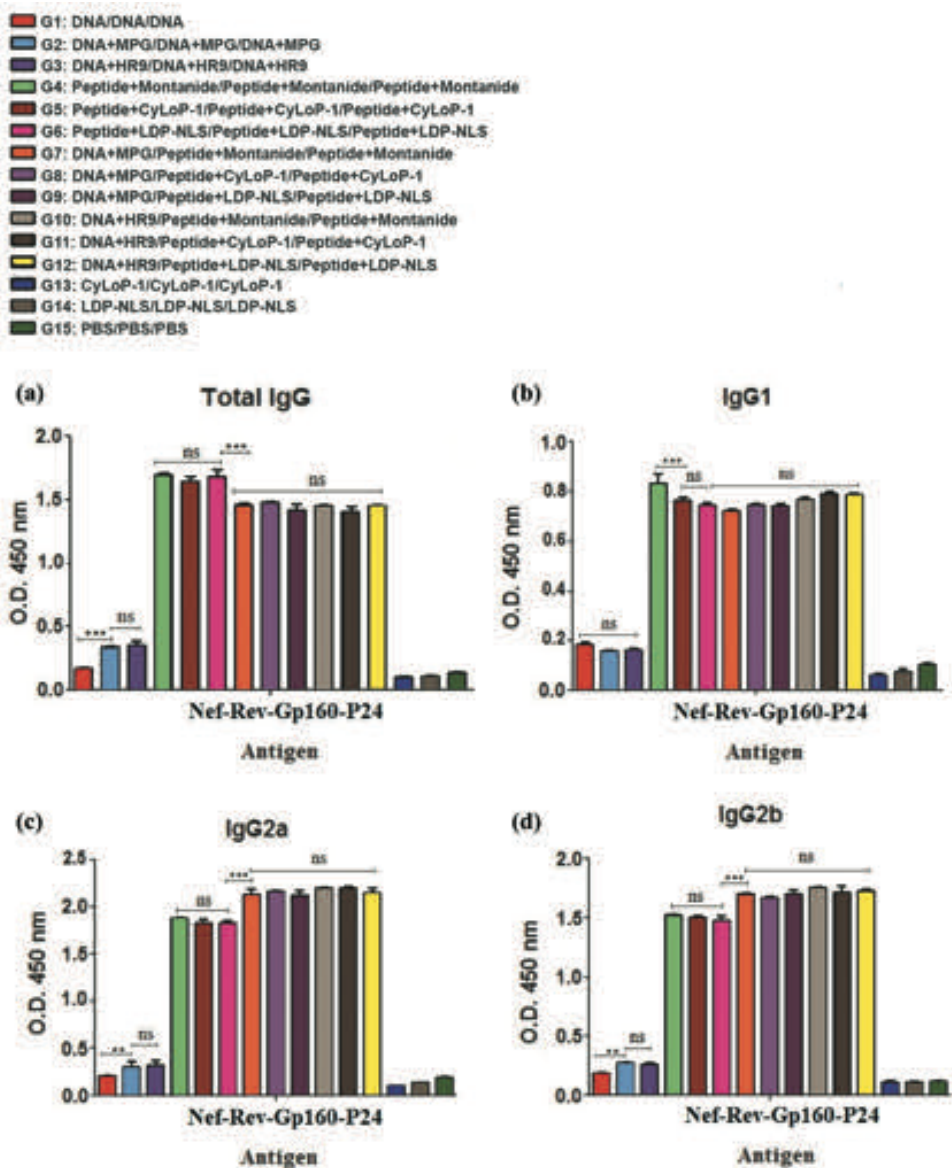


Figure 7. Evaluation of the total IgG (a), IgG1 (b), IgG2a (c) and IgG2b (d) antibodies against Nef-Rev-Gp160-P24 antigen in the sera of immunized mice using ELISA. All analyses were performed in duplicate for each sample (ns: non-significant; * $p < .05$; ** $p < .01$; *** $p < .001$).

heterologous DNA+MPG or HR9 prime/rNef-Rev-Gp160-P24 polypeptide+LDP-NLS boost (G9 and G12, respectively) than other groups (Figure 8d, $p < .01$). Additionally, the homologous polypeptide regimens (G4-G6) showed similar levels of Granzyme B ($p > .05$; Figure 8d). Moreover, there was a significant difference between group receiving the naked DNA (G1) and groups receiving homologous DNA+ MPG or HR9 (G2 and G3, $p < .001$).

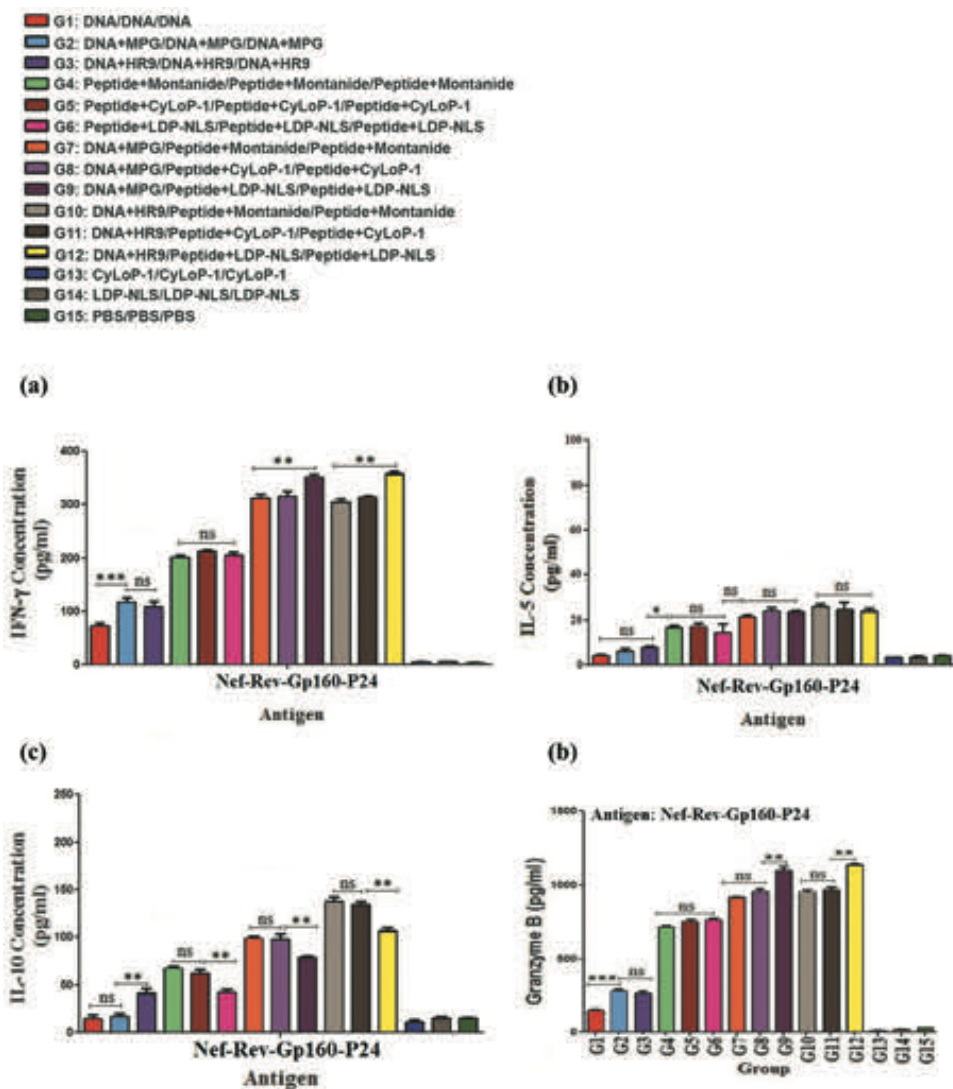


Figure 8. Evaluation of IFN- γ (A), IL-10 (B), IL-5 (C) and Granzyme B (D) secretion in immunized groups with the Nef-Rev-Gp160-P24 constructs in various formulations using ELISA. All analyses were performed in duplicate for each sample (ns: non-significant; * $p < .05$; ** $p < .01$; *** $p < .001$).

No significant difference was detected between groups that received DNA delivered by MPG or HR9 peptides (G2 and G3, $p > .05$).

Discussion

The final goal of HIV vaccine design needs novel strategies to stimulate strong cellular and humoral immunity (Abdulla et al. 2019). There are many multiepitope vaccines versus different viruses (e.g., Dengue virus (Ali et al. 2017), Hepatitis C virus (Ikram et al. 2018; Nosrati et al. 2017), Zika virus (Kumar Pandey et al. 2018), and Ebola virus (Bazhan et al.

2019)). Some reports suggested that the design of new vaccines based on a variety of immunogenic epitopes originated from the HIV-1 regulatory and structural proteins were more immunogenic than each of them, individually (Ahmed et al. 2016; Reguzova et al. 2015; Vardas et al. 2012). In this study, HIV-1 Nef, Rev, Gp160, and P24 proteins were chosen to design a novel multiepitope construct because of their major roles in the viral pathogenesis. To reach this aim, the full length of P24 involving the conserved CTL epitopes (Bolesta et al. 2005) and the conserved epitopes of Nef, Rev and Gp160 with the highest MHC class I and II binding scores were determined by immunoinformatics programs. Hence, epitope selection parameters such as immunogenicity, toxicity, allergenicity, hemolytic activity, cross-reactivity, CPP potency and interaction similarity with human and mouse HLA-alleles by molecular docking led to the selection of longer epitopes comprising overlapping multiple T- and B-cell epitopes. Thus, we selected four CTL epitopes derived from Rev protein (such as Rev₈₋₁₇, Rev₁₄₋₂₃, Rev₄₃₋₅₂, Rev₅₃₋₆₃) based on immunoinformatics analysis. Then, we designed a novel multiepitope construct using a set of overlapping CTL and HTL epitopes derived from four proteins. Long peptides induced more efficient immune responses than short peptides (Kardani et al. 2019). On the other hand, it is not clear whether synthetically designed multiepitope constructs containing T- and/or B-cell epitopes, can be processed and presented properly to generate specific immunity. Therefore, an important step in the improvement of multiepitope-based vaccine is predicting TAP transport and proteasomal cleavage. Based on the results of the IEDB database, it seems that all selected epitopes containing CD8⁺ and CD4⁺ T-cell epitopes are available for immune response during antigen processing and presentation by professional antigen-presenting cells (APCs). Moreover, it was confirmed that choosing an appropriate linker can significantly improve antigen presentation compared to the absence of linker (Pandey et al. 2018; Kumar Pandey et al. 2018; Meza et al. 2017). Therefore, for designing an efficient multiepitope subunit vaccine candidate, AAY linker with low immunogenicity was considered as proteasomal cleavage spacer of the selected epitopes. Almeida *et al.* developed an HIV-1 DNA vaccine encoding highly conserved peptides that showed cross-clade T cell responses and IFN- γ secretion in BALB/c mice (Almeida et al. 2012). The CombiHIVvac candidate vaccine against HIV-1 containing two synthetic polyepitope immunogens such as TBI (Env and Gag epitopes) and TCI (Env, Gag, Pol and Nef epitopes) was safe and induced the HIV-specific immunity in Phase I clinical trials (Karpenko et al. 2016).

Low immunogenicity of the multiepitope subunit vaccine was an important drawback of epitope-based vaccine strategy. Some studies recommended the use of delivery systems and prime/boost strategies to overcome this problem (Kuck et al. 2006). CPPs were utilized for delivery of different therapeutic molecules *in vitro* and *in vivo*. Some CPPs such as MPG or HR9 could transfer nucleic acids into the cells via electrostatic interaction (Liu et al. 2015; Morris et al. 1999; Ramsey and Flynn 2015). On the other hand, Ponnappan *et al.* indicated that CyLoP-1 and LDP-NLS CPPs deliver effectively proteins into mammalian cells (Ponnappan et al. 2017; Ponnappan and Chugh 2017). Herein, we applied four cell-penetrating peptides including MPG and HR9 for DNA delivery at certain N/P ratios, and CyLoP-1 and LDP-NLS for polypeptide delivery at certain molar ratio as used in our previous study (Namazi et al. 2019). Based on the flow cytometry and fluorescent microscopy results of the transfected HEK-293 T cells with MPG/DNA ($39.11\% \pm 0.67$) and HR9/DNA ($28.08\% \pm 0.42$), a significant difference was observed between the potency of MPG and HR9 to penetrate cargo into the cells. Higher penetrating ability of MPG might be as

consequence of method of cellular uptake and high positively charged spherical nanoparticles (Yoo et al. 2011).

On the other hand, prime-boost strategies were known as a main technique to induce robust CTL responses. Heterologous prime-boost vaccination is usually more effective than sequential homologous vaccinations in magnitude and quality of immune responses (De Rose et al. 2015). Several factors can modulate immune outcomes following prime-boost vaccination approach including route of administration, vaccine vectors, candidate antigens, and adjuvants. In this study, we utilized three different vaccination strategies including homologous DNA, homologous polypeptide, and heterologous DNA/polypeptide regimens to evaluate their immunogenicity in BALB/c mice. Herein, we observed that groups (G9 and G12) immunized with heterologous prime-boost regimens (pcDNA3.1-*nef-rev-gp160-p24* + MPG or HR9 prime followed by rNef-Rev-Gp160-P24 polypeptide + LDP-NLS boost) could significantly produce higher levels of IFN- γ and Granzyme B and lower levels of IL-10 than other groups. On the other hand, higher levels of IgG2a and IgG2b were observed in all heterologous prime-boost regimens (G7-G12) than homologous DNA or protein regimens (G1-G6). The groups receiving the homologous DNA + MPG/HR9 regimens could significantly increase the anti-rNef-Rev-Gp160-P24 antibody responses compared to the naked DNA which can be as a result of forming potential nanoparticles with acceptable size and positive charge to deliver the cargos through the cell membrane. Based on our present data, we concluded that the homologous immunizations typically increased the levels of total IgG, where the heterologous prime-boost immunizations enhanced the levels of anti-rNef-Rev-Gp160-P24 cytophilic antibodies (IgG2a and IgG2b) and proinflammatory Th1 cytokine (IFN- γ) and Granzyme B in mice. Cristillo *et al.*, showed that a polyvalent DNA prime/protein boost vaccine including HIV-1 env, gag and gp120 proteins in QS-21 could increase cellular immunity mediated by CTLs and T-helper 1 cells in macaques and mice (Cristillo et al. 2006). As reported, Th1 cells which produce IFN- γ , IL-2, and tumor necrosis factor (TNF)- α were known to promote cellular immunity especially during intracellular infections, whereas Th2 cells which produce IL-4, IL-5, IL-6, IL-9, IL-10 and IL-13 promote humoral immunity and antibody production. Thus, the balance of these cytokines determines Th1 or Th2 activity (Kühn et al. 1993; Ng et al. 2003; Sabat et al. 2010; Schoenborn and Wilson 2007). Our study also indicated that the ratios of the IFN- γ /IL-5 and IFN- γ /IL-10 are higher in test groups compared to control groups indicating the direction of immune responses toward Th1 activity.

Other major point is the importance of Rev regulatory protein as an antigen candidate in vaccine design. As known, HIV-1 Rev protein helps the transportation of viral RNA without processing from nucleus to cytoplasm for the translation process (Arya et al. 2015; Nabel et al. 2011). Recent studies showed that the CD8⁺ cytotoxic T cell (CTL) activity against Tat and Rev proteins could control HIV-1 load (Verrier et al. 2002). Moreover, the immunogenicity of DNA vectors harboring HIV-1 *nef*, *tat* and *rev* genes individually showed that the pBN-*nef* construct induced humoral and cellular immunity using intramuscular and intradermal delivery. In contrast, the pBN-*rev* construct only induced the CTL responses and the pBN-*tat* construct did not elicit any effective immune responses (Tähtinen et al. 2001). The DNA vectors encoding the HIV-1 Env and Rev proteins stimulated significantly antigen-specific antibodies and suppressed HIV-1 infection in mouse, rabbit, or macaque, as well (Okuda et al. 1995).

Herein, our results revealed that the use of multiepitope antigens, CPPs, and heterologous regimens simultaneously could increase cellular immunity and antibodies as a potential approach for development of a potent HIV-1 vaccine.

In summary, the present findings indicated that rNef-Rev-Gp160-P24 polypeptide can be considered potentially useful as a multiepitope-based vaccine candidate against HIV-1 infection. Thus, further investigation will be needed to realize whether anti-HIV-1 immune responses including antibody and cytokines against polypeptide are efficient in reduction of HIV-1 infection in animal model (*e.g.*, macaque). Moreover, the proportion of CD4⁺ T cells or CD8⁺ T cells producing cytokines will be determined in the best groups with the highest levels of IgG2a, IFN- γ and Granzyme B in near future.

Author contribution

All authors contributed significantly to this study.

Conceived and designed the experiments: SHS, AB

Performed the experiments: SHS, KK, AM

Analyzed the data: SHS, AB

Contributed reagents/materials/analysis tools: KK, AM

Wrote the manuscript: SHS, KK, AM

Edited and reviewed the manuscript: SHS, KK, AM, AB

Declaration of Competing Interest

The authors have declared that there is no conflict of interest.

Funding

This study was supported by Pasteur Institute of Iran (proposal code: 1070; ethical code: IR.PII.REC.1397.024).

References

- Abdulla F, Adhikari UK, Uddin MK. 2019. Exploring T and B-cell epitopes and designing multi-epitope subunit vaccine targeting integration step of HIV-1 lifecycle using immunoinformatics approach. *Microb Pathog.* 137:103791.
- Addo MM, Altfeld M, Rosenberg ES, Eldridge RL, Philips MN, Habeeb K, Khatri A, Brander C, Robbins GK, Mazzara GP, et al. 2001. The HIV-1 regulatory proteins Tat and Rev are frequently targeted by cytotoxic T lymphocytes derived from HIV-1-infected individuals. *Proc Natl Acad Sci.* 98(4):1781–86.
- Ahmed T, Borthwick NJ, Gilmour J, Hayes P, Dorrell L, Hanke T. 2016. Control of HIV-1 replication in vitro by vaccine-induced human CD8⁺ T cells through conserved subdominant Pol epitopes. *Vaccine.* 34(9):1215–24.
- Ali M, Pandey RK, Khatoun N, Narula A, Mishra A, Prajapati VK. 2017. Exploring dengue genome to construct a multi-epitope based subunit vaccine by utilizing immunoinformatics approach to battle against dengue infection. *Sci Rep.* 7(1):1–3.
- Almeida RR, Rosa DS, Ribeiro SP, Santana VC, Kallas EG, Sidney J, Sette A, Kalil J, Cunha-Neto E. 2012. Broad and cross-clade CD4⁺ T-cell responses elicited by a DNA vaccine encoding highly conserved and promiscuous HIV-1 M-group consensus peptides. *PLoS One.* 7(9):e45267.

- Apostólico JDS, Lunardelli VAS, Yamamoto MM, Souza HFS, Cunha-Neto E, Boscardin SB, Rosa DS. 2017. Dendritic cell targeting effectively boosts T cell responses elicited by an HIV multiepitope DNA vaccine. *Front Immunol.* 8:101.
- Arya S, Lal P, Singh P, Kumar A. 2015. Recent advances in diagnosis of HIV and future prospects. *Indian J Biotechnol.* 14:9–18.
- Bazhan SI, Antonets DV, Karpenko LI, Oreshkova SF, Kaplina ON, Starostina EV, Dudko SG, Fedotova SA, Ilyichev AA. 2019. *In silico* designed Ebola virus T-cell multi-epitope DNA vaccine constructions are immunogenic in mice. *Vaccines.* 7(2):34.
- Black M, Trent A, Tirrell M, Olive C. 2010. Advances in the design and delivery of peptide subunit vaccines with a focus on toll-like receptor agonists. *Expert Rev Vaccines.* 9(2):157–73.
- Boffito M, Fox J, Bowman C, Orkin C, Wilkins E, Jackson A, Pleguezuelos O, Robinson S, Stoloff GA, Caparrós-Wanderley W. 2013. Safety, immunogenicity and efficacy assessment of HIV immunotherapy in a multi-centre, double-blind, randomised, Placebo-controlled Phase Ib human trial. *Vaccine.* 31(48):5680–86.
- Bolesta E, Gzyl J, Wierzbicki A, Kmiecik D, Kowalczyk A, Kaneko Y, Srinivasand A, Kozbora D. 2005. Clustered epitopes within the Gag-Pol fusion protein DNA vaccine enhance immune responses and protection against challenge with recombinant vaccinia viruses expressing HIV-1 Gag and Pol antigens. *Virology.* 332(2):467–79.
- Chen C, Li Z, Huang H, Suzek BE, Wu CH. 2013. A fast peptide match service for UniProt knowledgebase. *Bioinformatics.* 29(21):2808–09.
- Chiarella P, Massi E, De Robertis M, Fazio VM, Signori E. 2009. Recent advances in epitope design for immunotherapy of cancer. *Recent Pat Anti-Cancer Drug Discovery.* 4(3):227–40.
- Cristillo AD, Wang S, Caskey MS, Unangst T, Hocker L, He L, Hudacik L, Whitney S, Keen T, Chou TW. 2006. Preclinical evaluation of cellular immune responses elicited by a polyvalent DNA prime/protein boost HIV-1 vaccine. *Virology.* 346(1):151–68.
- De Rose R, Kent SJ, Ranasinghe C. 2015. Prime-boost vaccination: impact on the HIV-1 vaccine field. In: *Novel approaches and strategies for biologics, vaccines and cancer therapies.* The University of Melbourne, Academic Press; p. 289–313. doi: [10.1016/B978-0-12-416603-5.00012-2](https://doi.org/10.1016/B978-0-12-416603-5.00012-2).
- Deshayes S, Gerbal-Chaloin S, Morris MC, Aldrian-Herrada G, Charnet P, Divita G, Heitz F. 2004. On the mechanism of non-endosomal peptide-mediated cellular delivery of nucleic acids. *Biochim Et Biophys Acta (Bba)-biomembr.* 1667(2):141–47.
- DeVico AL, Gallo RC. 2004. Control of HIV-1 infection by soluble factors of the immune response. *Nat Rev Microbiol.* 2(5):401–13.
- Dhanda SK, Gupta S, Vir P, Raghava GP. 2013a. Prediction of IL4 inducing peptides. *Clin Dev Immunol.* 2013:1–9.
- Dhanda SK, Vir P, Raghava GP. 2013b. Designing of interferon-gamma inducing MHC class-II binders. *Biol Direct.* 8(1):30.
- Falk K, Rötzschke O, Stevanović S, Jung G, Rammensee HG. 1991. Allele-specific motifs revealed by sequencing of self-peptides eluted from MHC molecules. *Nature.* 351(6324):290–96.
- Gasteiger E, Hoogland C, Gattiker A, Wilkins MR, Appel RD, Bairoch A. 2005. Protein identification and analysis tools on the ExPASy server. In: *The proteomics protocols handbook.* The Springer Protocols Handbooks book series (SPH). Humana press; p. 571–607.
- Gautam A, Chaudhary K, Kumar R, Raghava GP. 2015. Computer-aided virtual screening and designing of cell-penetrating peptides. In: *Cell-penetrating peptides.* The Methods in Molecular Biology book series (MIMB, Vol. 1324), Springer. New York (NY): Humana press; p. 59–69.
- Gautam A, Chaudhary K, Singh S. 2014. Hemolytik: a database of experimentally determined hemolytic and non-hemolytic peptides. *Nucleic Acids Res.* 42(D1):D444–9.
- Gonzalez-Rabade N, McGowan EG, Zhou F, Ralph Bock MSM, Dix PJ, Gray JC, Ma JKC. 2011. Immunogenicity of chloroplast-derived HIV-1 p24 and a p24-Nef fusion protein following subcutaneous and oral administration in mice. *Plant Biotechnol J.* 9(6):629–38.
- Gros E, Deshayes S, Morris MC, Aldrian-Herrada G, Depollier J, Heitz F, Divita G. 2006. A non-covalent peptide-based strategy for protein and peptide nucleic acid transduction. *Biochim Et Biophys Acta (Bba)-biomembr.* 1758(3):384–93.

- Gupta S, Kapoor P, Chaudhary K, Gautam A, Kumar R, Raghava GP. 2013. *In silico* approach for predicting toxicity of peptides and proteins. *PLoS One*. 8(9):e73957.
- Hebditch M, Carballo-Amador MA, Charonis S, Curtis R, Warwicker J. 2017. Protein-Sol: a web tool for predicting protein solubility from sequence. *Bioinformatics*. 33(19):3098–100.
- Ikram A, Zaheer T, Awan FM, Obaid A, Naz A, Hanif R, Zafar Paracha R, Ali A, Naveed A, Janjua HA. 2018. Exploring NS3/4A, NS5A and NS5B proteins to design conserved subunit multi-epitope vaccine against HCV utilizing immunoinformatics approaches. *Sci Rep*. 8(1):1–4.
- Kardani K, Bolhassani A, Namvar A. 2020. An overview of *in silico* vaccine design against different pathogens and cancer. *Expert Rev Vaccines*. 19(8):699–726.
- Kardani K, Hashemi A, Bolhassani A. 2019. Comparison of HIV-1 Vif and Vpu accessory proteins for delivery of polyepitope constructs harboring Nef, Gp160 and P24 using various cell penetrating peptides. *PLoS One*. 14(10):e0223844.
- Karpenko LI, Bazhan SI, Bogryantseva MP, Ryndyuk NN, Ginko ZI, Kuzubov VI, Lebedev LR, Kaplina ON, Reguzova A, Ryzhikov AB, et al. 2016. Results of phase I clinical trials of a combined vaccine against HIV-1 based on synthetic polyepitope immunogens. *Russ J Bioorg Chem*. 42(2):170–82.
- Khairkhah N, Namvar A, Kardani K, Bolhassani A. 2018. Prediction of cross-clade HIV-1 T-cell epitopes using immunoinformatics analysis. *Proteins Struct Funct Bioinf*. 86(12):1284–93.
- Kuck D, Lau T, Leuchs B, Kern A, Müller M, Gissmann L, Kleinschmidt JA. 2006. Intranasal vaccination with recombinant adeno-associated virus type 5 against human papillomavirus type 16 L1. *J Virol*. 80(6):2621–30.
- Kühn R, Löhler J, Rennick D, Rajewsky K, Müller W. 1993. Interleukin-10-deficient mice develop chronic enterocolitis. *Cell*. 75:263–74.
- Kumar Pandey R, Ojha R, Mishra A, Kumar Prajapati V. 2018. Designing B- and T-cell multi-epitope based subunit vaccine using immunoinformatics approach to control Zika virus infection. *J Cell Biochem*. 119(9):7631–42.
- Leal L, Lucero C, Gatell JM, Gallart T, Plana M, García F. 2017. New challenges in therapeutic vaccines against HIV infection. *Expert Rev Vaccines*. 16(6):587–600.
- Liu BR, Chen HH, Chan MH, Huang YW, Aronstam RS, Lee HJ. 2015. Three arginine-rich cell-penetrating peptides facilitate cellular internalization of red-emitting quantum dots. *J Nanosci Nanotechnol*. 15(3):2067–78.
- Liu BR, Huang YW, Winiarz JG, Chiang HJ, Lee HJ. 2011. Intracellular delivery of quantum dots mediated by a histidine- and arginine-rich HR9 cell-penetrating peptide through the direct membrane translocation mechanism. *Biomaterials*. 32(13):3520–37.
- Meza B, Ascencio F, Sierra-Beltrán AP, Torres J, Angulo C. 2017. A novel design of a multi-antigenic, multistage and multi-epitope vaccine against *Helicobacter pylori*: an *in silico* approach. *Infect Genet Evol*. 49:309–17.
- Morris MC, Chaloin L, Méry J, Heitz F, Divita G. 1999. A novel potent strategy for gene delivery using a single peptide vector as a carrier. *Nucleic Acids Res*. 27(17):3510–17.
- Nabel GJ, Kwong PD, Mascola JR. 2011. Progress in the rational design of an AIDS vaccine. *Phil Trans R Soc B*. 366:2759–65.
- Namazi F, Bolhassani A, Sadat SM, Irani S. 2019. Delivery of HIV-1 polyepitope constructs using cationic and amphipathic cell penetrating peptides into mammalian cells. *Curr HIV Res*. 17(6):408–28.
- Ng PC, Li K, Wong RPO, Chui K, Wong E, Li G, Fok TF. 2003. Proinflammatory and anti-inflammatory cytokine responses in preterm infants with systemic infections. *Arch Dis Child Fetal Neonatal Ed*. 88:F209–13.
- Nosrati M, Mohabatkar H, Behbahani M. 2017. A novel multi-epitope vaccine for cross protection against hepatitis C virus (HCV): an immunoinformatics approach. *Res Mol Med*. 5(1):17–26.
- Okuda K, Bukawa H, Hamajima K, Kawamoto S, Sekigawa K, Yamada Y, Tanaka S, Ishi N, Aoki I, Nakamura M. 1995. Induction of potent humoral and cell-mediated immune responses following direct injection of DNA encoding the HIV type 1 *env* and *rev* gene products. *AIDS Res Hum Retroviruses*. 11:933–43.

- Pandey RK, Ojha R, Aathmanathan VS, Krishnan M, Prajapati VK. 2018. Immunoinformatics approaches to design a novel multi-epitope subunit vaccine against HIV infection. *Vaccine*. 36 (17):2262–72.
- Ponnappan N, Budagavi DP, Chugh A. 2017. CyLoP-1: membrane-active peptide with cell-penetrating and antimicrobial properties. *Biochim Et Biophys Acta (Bba)-biomembr*. 1859 (2):167–76.
- Ponnappan N, Chugh A. 2017. Cell-penetrating and cargo-delivery ability of a spider toxin-derived peptide in mammalian cells. *Eur J Pharm Biopharm*. 114:145–53.
- Ramsey JD, Flynn NH. 2015. Cell-penetrating peptides transport therapeutics into cells. *Pharmacol Ther*. 154:78–86.
- Ranasinghe S, Soghoian DZ, Lindqvist M, Ghebremichael M, Donaghey F, Carrington M, Seaman MS, Kaufmann DE, Walker BD, Porichis F. 2016. HIV-1 antibody neutralization breadth is associated with enhanced HIV-specific CD4⁺ T cell responses. *J Virol*. 90(5):2208–20.
- Reguzova A, Antonets D, Karpenko L, Ilyichev A, Maksyutov R, Bazhan S. 2015. Design and evaluation of optimized artificial HIV-1 poly-T cell-epitope immunogens. *PLoS One*. 10(3): e0116412.
- Rosa DS, Ribeiro SP, Almeida RR, Mairena EC, Posto E, Kalil J, Cunha-Neto E. 2011. A DNA vaccine encoding multiple HIV CD4 epitopes elicits vigorous polyfunctional, long-lived CD4⁺ and CD8⁺ T cell responses. *PLoS One*. 6(2):e16921.
- Sabat R, Grütz G, Warszawska K, Kirsch S, Witte E, Wolk K, Geginat J. 2010. Biology of interleukin-10. *Cytokine Growth Factor Rev*. 21:331–44.
- Saha S, Raghava GP. 2006a. AlgPred: prediction of allergenic proteins and mapping of IgE epitopes. *Nucleic Acids Res*. 34(2):W202–9.
- Saha S, Raghava GP. 2006b. Prediction of continuous B-cell epitopes in an antigen using recurrent neural network. *Proteins Struct Funct Bioinf*. 65(1):40–48.
- Sahni AK, Nagendra A. 2004. HIV vaccine strategies: an update. *Med J Armed Forces India*. 60 (2):157.
- Schoenborn JR, Wilson CB. 2007. Regulation of interferon- γ during innate and adaptive immune responses. Washington, USA: Adv Immunol Academic Press; p. 41–101.
- Schuler MM, Nastke MD, Stevanović S. 2007. SYFPEITHI. In: Immunoinformatics. Springer Protocol. Humana Press; p. 75–93.
- Slingluff CL. 2011. The present and future of peptide vaccines for cancer: single or multiple, long or short, alone or in combination? *Cancer J*. 17(5):343.
- Spira S, Wainberg MA, Loomba H, Turner D, Brenner BG. 2003. Impact of clade diversity on HIV-1 virulence, antiretroviral drug sensitivity and drug resistance. *J Antimicrob Chemother*. 51 (2):229–40.
- Tähtinen M, Strengell M, Collings A, Pitkänen J, Kjerrström A, Hakkarainen K, Peterson P, Kohleisen B, Wahren B, Ranki A, et al. 2001. DNA vaccination in mice using HIV-1 *nef*, *rev* and *tat* genes in self-replicating pBN-vector. *Vaccine*. 19:2039–47.
- Vardas E, Stanescu I, Leinonen M, Ellefsen K, Pantaleo G, Valtavaara M, Ustav M, Reijonen K. 2012. Indicators of therapeutic effect in FIT-06, a phase II trial of a DNA vaccine, GTU[®]-Multi-HIVB, in untreated HIV-1 infected subjects. *Vaccine*. 30(27):4046–54.
- Verrier B, Le Grand R, Ataman-Önal Y, Terrat C, Guillon C, Durand PY, Hurtrel B, Aubertin AM, Sutter G, Erfle V, et al. 2002. Evaluation in *rhesus macaques* of Tat and rev-targeted immunization as a preventive vaccine against mucosal challenge with SHIV-BX08. *DNA Cell Biol*. 21(9):653–58.
- Yoo JW, Doshi N, Mitragotri S. 2011. Adaptive micro and nanoparticles: temporal control over carrier properties to facilitate drug delivery. *Adv Drug Delivery Rev*. 63(14–15):1247–56.
- Zhang Q, Wang P, Kim Y, Haste-Andersen P, Beaver J, Bourne PE, Bui HH, Buus S, Frankild S, Greenbaum J, et al. 2008. Immune epitope database analysis resource (IEDB-AR). *Nucleic Acids Res*. 36(2):W513–8.